

# Pillared laponite clays-supported palladium catalysts for the complete oxidation of benzene

Li Jinjun, Jiang Zheng, Hao Zhengping\*, Xu Xiuyan, Zhuang Yahui

*Research Center for Eco-Environmental Sciences, Chinese Academy of Sciences, Beijing 100085, China*

Received 13 March 2004; received in revised form 17 August 2004; accepted 20 August 2004

## Abstract

Zr-, Ce-, and Al-pillared laponite clays (Al-Lap, Ce-Lap, Zr-Lap) were prepared and used as supports of palladium catalysts for the complete oxidation of benzene. The pillared clays and the supported Pd catalysts were characterized by N<sub>2</sub> adsorption/desorption, differential scanning calorimetry (DSC), hydrogen chemisorption and temperature-programmed reduction (TPR) techniques. The specific surface areas of the pillared clays exceed 430 m<sup>2</sup>/g, and the pore diameters are greater than 4 nm. DSC analysis revealed that the pillared clays have higher thermal stability in comparison with the parent clay. Palladium catalysts supported on the pillared clays are much more active than those supported on conventional alumina. Pd/Zr-Lap, in particular, could catalyze the complete oxidation of benzene at a temperature as low as 210 °C. The effect of calcination temperature on the catalytic activity was investigated. The optimal calcination temperature was found to be 400 °C for Pd/Al-Lap catalysts, and 600 °C for Pd/Zr-Lap and Pd/Ce-Lap catalysts. At optimal calcination temperatures, palladium crystallites of proper size could be formed in pillared clays and showed a higher activity than those calcined at other temperatures.

© 2004 Elsevier B.V. All rights reserved.

**Keywords:** Pillared clays; VOCs; Benzene; Catalytic oxidation; Palladium catalysts

## 1. Introduction

Volatile organic compounds (VOCs) cause environmental concerns about their toxicity and malodor, as well as on their role in photochemical formation of ozone and smog in the boundary layer [1]. Although some VOCs have their origin from vegetation, but abatement of anthropogenic sources remains to be a major concern. Many techniques have been developed for the mitigation of industrial VOCs emissions in the last few decades. Among them, incineration is a convenient way to convert VOCs into nontoxic carbon dioxide and water. However, conventional thermal incineration requires an operating temperature as high as 1000 °C, and consumes significant amounts of energy. Furthermore, toxic by-products, such as dioxin, dibenzofuran and nitrogen oxides, could be formed in such processes if the conditions are not

carefully controlled. On the other hand, catalytic oxidation can be conducted at much lower temperatures (usually less than 500 °C), and the selectivity of the catalytic reaction could be effectively controlled. Thus, catalytic complete oxidation has been recognized as one of the most promising techniques for VOCs abatement, and has been extensively studied [2,3]. Much attention has been paid to the improvement of catalyst activity that could prompt the complete oxidation of VOCs at rather low temperatures. The support materials may play important roles in the catalytic reactions either by providing large surface areas to disperse the active metals, or by participating in the reactions as a catalyst promoter. Pillared interlayered clays (PILCs) are interesting porous materials that can be used as catalysts or catalyst supports due to their peculiar properties and structures [4,5]. In recent years, intensive studies on the catalytic applications of pillared clays have been reported [6]. Synthetic laponite clays are known of their superior porosity and excellently high surface areas [7–9]. Hao et al. [9] found Zr-pillared laponite clay is a good

\* Corresponding author. Tel.: +86 10 6284 9194; fax: +86 10 6292 3564.  
E-mail address: [zpinghao@mail.rcees.ac.cn](mailto:zpinghao@mail.rcees.ac.cn) (H. Zhengping).

support of nickel catalysts for methane reforming with carbon dioxide. However, it has not been employed for VOCs abatement.

In the present work, Al-, Ce- and Zr-pillared laponite clays (Al-Lap, Ce-Lap, Zr-Lap) were prepared and used as supports of palladium catalysts for the complete oxidation of benzene. Both the supports themselves and the supported catalysts were characterized by  $N_2$  adsorption/desorption, TPR and DSC techniques. The promoting effect of the pillars on the activity of the palladium catalysts was examined, and the influence of calcination temperature on the catalyst activity was investigated in detail.

## 2. Experimental

### 2.1. Catalyst preparation

Laponite clay was supplied by Fernz Specialty Chemicals, Australia. The nonionic PEO surfactant Tergitol type 15-S-9 was procured from the Sigma Chemical Co. Zr-, Ce- and Al-pillared laponite clays were prepared by a procedure similar to that was reported in the literature [7,8].

For the preparation of Zr-pillared laponite clay, 19.34 g of  $ZrOCl_2 \cdot 8H_2O$  was dissolved in 120 mL of water, and the solution was refluxed for 1 h to form the pillaring solution. Meanwhile, 5 g of laponite clay was dispersed in 240 mL of water under stirring to get a transparent colloidal solution, then 10 g of surfactant Tergitol type 15-S-9 was added and stirred for 2 h. Subsequently, the refluxed pillaring solution was added, and the mixture was maintained at 90 °C for 48 h. Then it was centrifuged and the precipitate was washed by deionized water until it was free of chloride ions. The wet cake was dried and finally calcined at 550 °C for 20 h. The resultant sample was designated hereafter as Zr-Lap. The Ce-pillared laponite clay was prepared in a similar way as Zr-Lap with a pillaring solution containing 26.06 g of  $Ce(NO_3)_3 \cdot 6H_2O$ . The resultant sample was designated as Ce-Lap.

Regarding the preparation of Al-pillared laponite clay, the pillaring solution was prepared as described in the literature [10]. 265 ml of 0.5 M NaOH solution was dropped slowly into 415 mL of 0.2 M  $Al(NO_3)_3$  solution under continuous stirring, and the stirring was maintained for 2 h. Then the mixture was aged at room temperature for 24 h, thus forming the pillaring solution. Then the clay was pillared just as in the case of Zr-Lap preparation. The final sample was designated as Al-Lap.

Pillared laponite clays supported palladium catalysts with a loading of 0.3 wt.% were prepared by the incipient wetness impregnation method with an aqueous solution of  $PdCl_2$  as the metal precursor. The impregnated solids were dried at 120 °C overnight, calcined in muffle furnace at various temperatures from 300 °C to 700 °C for 5 h, then reduced in pure hydrogen at various temperatures from 300 °C to 600 °C for 3 h. The final catalysts were designated as Pd/*M*-Lap(*A–B*), where *M* stands for the pillar elements, and *A* and *B* are

the calcination and reduction temperatures, respectively. The acronyms were shortened to PML(*A–B*) in some tables and figures of this paper. For comparison, we also prepared palladium catalysts loaded on the parent laponite clay and on  $\gamma-Al_2O_3$ . These catalysts were calcined and reduced both at 500 °C, and designated as Pd/ $Al_2O_3$  and Pd/Lap, respectively.

### 2.2. Catalyst characterization

The textural properties of the samples were determined by nitrogen adsorption/desorption at liquid nitrogen temperature, using a gas sorption analyzer NOVA 1200. The samples were outgassed at 330 °C for 4 h before the measurements. The total pore volume was obtained at a relative pressure of  $P/P_0 = 0.99$ .

DSC analysis was conducted on Setaram Labsys-16. In each experiment, about 10 mg of sample was used, and the temperature was raised from 20 °C to 1000 °C with a heating rate of 10 °C/min under a nitrogen flow of 20 mL/min.

The dispersion of the supported palladium was determined by chemisorption of hydrogen at room temperature, assuming that the hydrogen atoms were adsorbed on all exposed palladium atoms with a H:Pd stoichiometric ratio of 1. The molar ratio of chemisorbed hydrogen atoms to the total palladium atoms H/Pd was used for the evaluation of the Pd dispersion. The mean crystallite sizes were estimated from the equation  $d$  (nm) =  $112/(\text{percentage of metal exposed})$  [11,12], assuming that the palladium crystallites were spherical in shape with a surface atom density of  $1.27 \times 10^9$  atoms/m<sup>2</sup>.

Temperature-programmed reduction (TPR) tests were carried out in a continuous flow quartz reactor, which was connected with a TCD detector. In each test, 0.2 g of catalyst was used, and the heating rate was 10 °C/min. Before each test, the catalyst was oxidized in air at 400 °C for 5 h.

### 2.3. Activity evaluation

Catalytic activity tests were performed in a continuous-flow fixed-bed reactor of i.d. 6 mm, which was placed in a tubular electric furnace equipped with a temperature programmer. In each test run, 0.4 g of catalyst (40–60 mesh) diluted with an appropriate amount of quartz beads was placed at the center of the reactor, above which a thermocouple was located to monitor reaction temperatures. Benzene was chosen as the representative of VOCs. A small air stream flowed through a boat-shaped saturator in ice-bath so that the air contained concentrated benzene vapor, then it was further diluted with another airflow before reaching the catalyst bed. And, the total flow rate was set at 320 mL/min with a benzene concentration of about 1050 ppm. The gas hourly space velocity (GHSV) was kept at about 20,000 h<sup>-1</sup>. An on-line gas chromatograph equipped with a FID detector was used to analyze benzene concentrations in the feed and effluent gas. Before each test, the temperature of the catalytic bed was raised to 130 °C under the feed stream and stabilized at that

Table 1  
Textural properties of the clays and  $\gamma$ -Al<sub>2</sub>O<sub>3</sub>

Sample	S <sub>BET</sub> <sup>a</sup> (m <sup>2</sup> /g)	V <sub>p</sub> <sup>b</sup> (cm <sup>3</sup> /g)	D <sub>p</sub> <sup>c</sup> (nm)
Laponite	315	0.23	2.9
Al-Lap	549	0.76	5.6
Ce-Lap	435	0.8	7.4
Zr-Lap	561	0.57	4.1
$\gamma$ -Al <sub>2</sub> O <sub>3</sub>	247	0.24	4.0

<sup>a</sup> BET specific surface areas.

<sup>b</sup> Total pore volumes are obtained at  $P/P_0 = 0.99$ .

<sup>c</sup> Average pore diameters.

temperature. Generally speaking, no benzene oxidation was observed at this temperature, and then the temperature of the catalyst bed was raised with a heating rate of 5 °C/min. The temperature was then kept constant for 3 min at each datum point prior to recording the benzene concentration in the effluent gas. A blank test conducted with only quartz beads in the reactor showed that the homogeneous reaction at a temperature less than 350 °C was negligible.

Long-term stability tests over several samples were carried out under conditions similar to the activity evaluation except that the concentration of benzene in the feed gas was increased to 2000 ppm. In each run, the catalytic bed was firstly heated to a temperature at which a conversion value of more than 95% was achieved, then decreased to a certain temperature and maintained constant at that temperature for about 70 h.

### 3. Results and discussion

#### 3.1. Characterization of the pillared clays

The textural properties of the clays and  $\gamma$ -Al<sub>2</sub>O<sub>3</sub> are presented in Table 1. The pillared clays have larger specific surface areas, total pore volume and average pore diameters in comparison with the parent clay. During the hydrothermal treatment, the polyoxycations in the solution could have been intercalated into the clay layers, and they were converted into metal oxide pillars after calcination with the silicate layers propped apart, leading to the alternation of the porosity of the clay [13,14]. Among the three pillared clays, Zr-Lap showed the highest specific surface area of 561 m<sup>2</sup>/g, but its total pore volume and average pore diameter were relatively lower than the other two pillared clays. Probably the properties of the polyoxycations in the pillaring solution affect profoundly the structure of the final pillared clay.

The DSC profiles of the pillared clays as well as the parent clay are shown in Fig. 1. In all the samples, two endothermic effects were observed. The first one occurred at temperatures below 200 °C could be assigned to the desorption of the adsorbed and hydration water molecules on the surface of the clay layers or on the pillars, while the second one at higher temperatures could be assigned to the removal of water formed by the condensation of structural hydroxyl

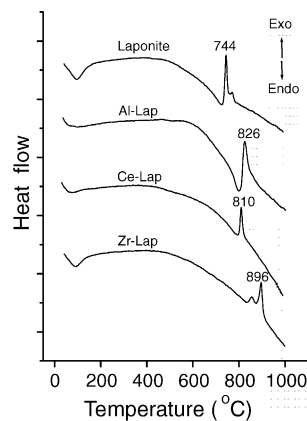


Fig. 1. DSC curves of various pillared clays and the parent clay.

groups [14]. An exothermic effect followed immediately the second endothermic effect in the higher temperature region. These two opposite effects took place at very similar temperatures, thus overlapping with each other. This exothermic effect could be attributed to the phase changes in the clays, which destroyed the clay structure completely, producing simple silicate [14]. The exothermic peak was centered at 744 °C, 826 °C, 810 °C and 896 °C for the parent clay, Al-Lap, Ce-Lap and Zr-Lap, respectively. Obviously, the introduced pillars have promoted the thermal stability of the clay. Zr-Lap, in particular, takes a phase transformation at a temperature about 150 °C higher than the parent clay.

#### 3.2. Dispersion of palladium on various supports

The H/Pd ratio and the calculated mean palladium particle size of various catalysts are listed in Table 2. The H/Pd ratio of both Zr- and Ce-based palladium catalysts appeared to be higher than that of Al-based catalyst when they were all calcined at 500 °C. Generally speaking, increasing the calcination temperature would decrease the dispersion of palladium except the Al-pillared palladium catalyst calcined at 300 °C, which showed a remarkably lower dispersion than those calcined at 400 °C and 500 °C. This might be explained by the retention of chlorine on the Pd/Al-Lap(300–300) catalyst due to the relatively low calcination and reduction temperatures. It is well known that chlorine inhibits the chemisorption of hydrogen atoms on noble metals [15,16], and that alumina could take up chlorine more readily [17,18].

#### 3.3. Temperature-programmed reduction (TPR) study of the catalysts

Fig. 2 displays the H<sub>2</sub>-TPR profiles of the Pd/Zr-Lap series of catalysts. The sole peak below 300 °C can be ascribed to the reduction of palladium oxide to metallic palladium for all samples. The reduction peak shifted toward a lower temperature with an increment of the calcination temperature. For the sample calcined at 500 °C, reduction started at 67 °C and reached a maximum at 106 °C. However, for the sample

Table 2  
Properties of the catalysts

Catalyst	Calcination temperature (°C)	Reduction temperatures (°C)	$S_{\text{BET}}$ (m <sup>2</sup> /g)	H/Pd <sup>a</sup>	$d^b$ (nm)	$T_{50}^c$ (°C)	$T_{90}$ (°C)
Pd/Ce-Lap	400	400	– <sup>e</sup>	0.833	1.34	265	300
	500	500	368	0.54	2.07	230	250
	600	600	332	0.455	2.46	205	230
	600	– <sup>d</sup>	–	–	–	320	360
	700	600	308	0.335	3.34	205	225
Pd/Zr-Lap	500	500	504	0.625	1.79	195	210
	600	600	474	0.506	2.21	180	195
	700	600	434	0.455	2.46	180	195
Pd/Al-Lap	300	300	–	0.297	3.77	285	310
	400	400	–	0.561	2.00	230	270
	500	500	479	0.453	2.47	245	270

<sup>a</sup> Molar ratio of adsorbed hydrogen atoms to the total palladium atoms.

<sup>b</sup> Calculated diameters of palladium crystallites based on the dispersion of Pd.

<sup>c</sup>  $T_{50}$  and  $T_{90}$  were the temperatures at which 50% and 90% of benzene were converted.

<sup>d</sup> The catalyst was calcined at 600 °C in air, but not reduced.

<sup>e</sup> Not measured.

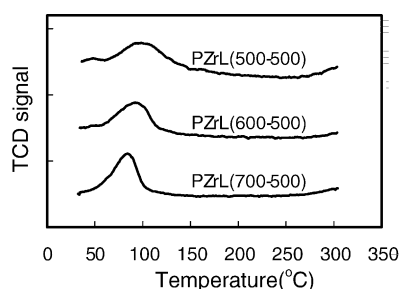


Fig. 2. TPR profiles of Pd/Zr-Lap catalysts calcined at various temperatures.

calcined at 700 °C, both the start-up temperature and the maximum of reduction peak shifted down to 50 °C and 88 °C, respectively. In addition, the reduction peak became higher but narrower with increasing the calcination temperature, indicating that the samples calcined at higher temperatures were reduced more quickly.

Fig. 3 displays the H<sub>2</sub>-TPR profiles of the Pd/Ce-Lap series of catalysts. The large peaks of the samples calcined at 400 °C and 500 °C could be attributed to the reduction of ceria, as these samples consumed much more hydrogen than

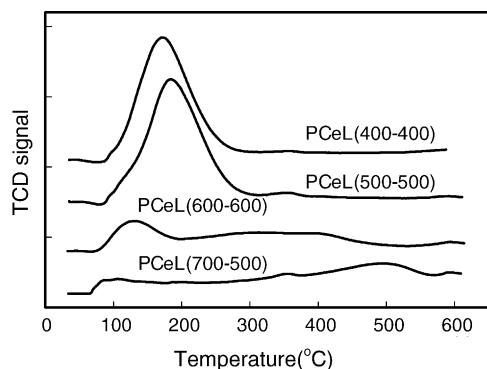


Fig. 3. TPR profiles of Pd/Ce-Lap catalysts calcined at various temperatures.

palladium oxide alone could consume. For the samples calcined at 600 °C and 700 °C, the reduction peaks were much lower in height but prolonged to much higher temperatures, and the reduction was not finished even at 600 °C. Apparently, there is a retardation of the ceria reduction with increasing calcination temperature. Typically, oxygen in the surface layer of ceria was reduced at a relatively lower temperature of about 500 °C, while the removal of the bulk oxygen occurred at a temperature higher than 800 °C [19,20]. It should be noticed that the reduction temperature of ceria in these catalysts was much lower than that of pure ceria. The promoted reduction of ceria in these samples could be attributed to the promoting effect of noble metal [21–24]. It has been reported that supported noble metals could activate hydrogen molecules and then spill the hydrogen atoms over onto the surface of ceria [25–27]. We suggest that the palladium species were in intimate contact with ceria when the catalysts were calcined at relatively lower temperatures, favoring the spillover of the hydrogen atoms. Thus ceria in samples calcined at lower temperatures could more easily be reduced.

### 3.4. Influence of calcination and reduction temperatures on the catalytic activity

The activity of the catalysts depends, to a great extent, on the temperature of calcination, as indicated in Fig. 4. The  $T_{50}$  and  $T_{90}$  temperatures, namely, temperatures for 50% and 90% of benzene conversion, are listed in Table 2. For the Al-pillared clay-based catalysts (Fig. 4a), the sample calcined at a moderate temperature of 400 °C showed the best catalytic activity, whereas for the other two pillared clay-based catalysts (Fig. 4b and c), the best activity was showed by the samples calcined at 600 °C and 700 °C. Lowering the calcination temperature would shift the conversion curves toward higher temperatures. As a rule, calcination at too high a temperature would often induce agglomeration of the noble metals, thus

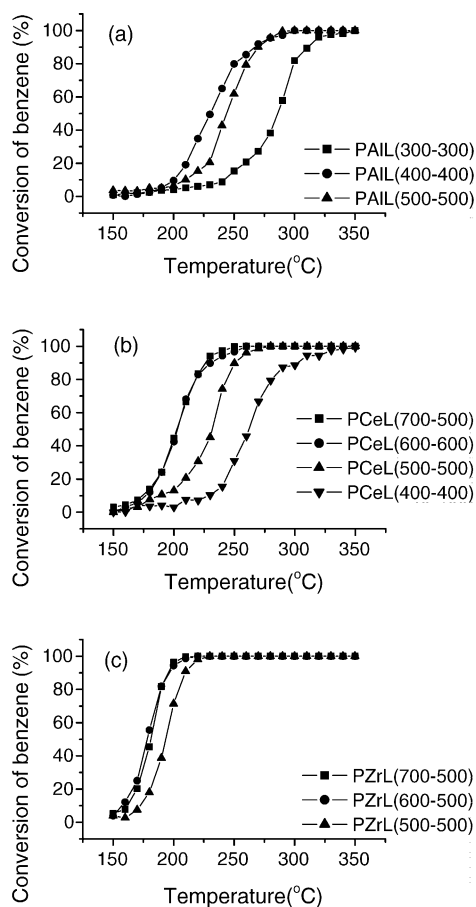


Fig. 4. Conversion curves for benzene oxidation over catalysts calcined at various temperatures. (a) Pd/Al-Lap; (b) Pd/Ce-Lap; (c) Pd/Zr-Lap.

resulting in a diminution of the catalyst activity. Remarkably, Ce- and Zr-pillared catalysts did not follow such a rule.

We also studied the influence of the reduction temperature on the catalyst activity. Fig. 5 shows the conversion curves of benzene oxidation over Pd/Ce-Lap catalysts calcined at 600 °C but reduced at various temperatures. The reduction treatment did have a positive effect on the catalysts. But, it is unlikely that the reduction temperature is the ruling factor determining the catalyst activity, as all the reduced catalysts gave almost the same conversion curves in spite of the difference in reduction temperature. Certain palladium oxide

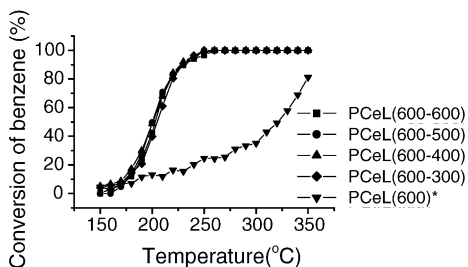


Fig. 5. Conversion curves for benzene oxidation over Pd/Ce-Lap catalysts calcined at 600 °C but reduced at various temperatures. \*PCeL(600) was the catalyst that was only calcined at 600 °C but not reduced.

species in a less oxidative state could be responsible for the activity of palladium catalysts in oxidation reactions [28–31]. In those cases, a surface redox cycle known as Mars-van Krevelen mechanism would be involved in catalytic oxidation reactions of hydrocarbons. In other words, the hydrocarbons were oxidized by depriving the oxygen atoms from palladium oxide species, and the reduced palladium was subsequently oxidized by oxygen again. If such a mechanism is applicable to benzene oxidation in our work, the reducibility of the palladium oxide species can be the main factor determining the catalyst activity. TPR tests of the Pd/Zr-Lap series of catalysts showed that the samples calcined at elevated temperature were more easily reduced, it is in good agreement with the activity of these catalysts (Fig. 2).

On the other hand, the elevated calcination temperature induced the growth of palladium crystallites, as indicated in Table 2. Samples with larger crystallite sizes were more active in the cases of Pd/Zr-Lap and Pd/Ce-Lap catalysts. This is contrary to Epling's findings [32] that Pd/ZrO<sub>2</sub> catalysts calcined at lower temperatures catalyzed the methane oxidation more efficiently than those calcined at higher temperatures, for higher temperature had caused severe sintering of palladium. As compared with our work, Epling's catalyst has a rather low specific area of 24.5 m<sup>2</sup>/g and a relatively high-Pd loading of 5 wt.%. Thus, the supported palladium atoms would possibly tend to form large crystallites more readily, and the surface areas of the active phases as well as the catalytic activity become reduced. Nevertheless, extremely small crystallite sizes could also bring about negative effects. According to Kundakovic [33], copper exists in the forms of either highly dispersed clusters or isolated copper ions on ceria or zirconia-supported copper catalysts with low loading (<5 at.%). Higher temperatures are required to reduce the copper with low loading than with moderate loading (less than 15 at.%). Other authors [34–36] reported that the ease of reduction of supported cobalt oxide diminished from larger to smaller particles. The ease and extent of the reduction depend upon the interaction between the metal oxide and the support, and weakening such interactions facilitates the reduction process. Meanwhile, the metal-support interaction becomes intensified with a decrement of the supported particle size. As a consequence, too strong an interaction, or alternatively, too small a metal oxide crystallite size, might bring about negative influence on the catalytic activities of oxidative catalysts. Pradier [37] studied the oxidation reaction of organic compounds on supported chromia catalysts, and found that the crystalline Cr<sub>2</sub>O<sub>3</sub> displayed a much higher catalytic activity than amorphous grafted species, which was in strong interaction with the support. Ji et al. [38] also found that for CO oxidation on Co/Al<sub>2</sub>O<sub>3</sub> catalysts, the activity increased with the decrease of metal-support interaction. We proposed that the supported catalysts exhibited the best performance when the sizes of the active crystallites fell into a certain range.

In our work, the catalysts possessed rather large surface areas as well as low loading of palladium, so it was possible

that the palladium species existed as either isolated atoms or small clusters, interacting strongly with the supports. Such a correlation was observed by other authors [36]: the interaction between the cobalt oxide species and  $\gamma$ -alumina support with high-surface areas ( $>300\text{ m}^2/\text{g}$ ) were very strong. Furthermore, the TPR profiles have indicated that the palladium species on the Pd/Ce-Lap catalysts calcined at low temperatures were in intimate contact with ceria, and this could also be viewed as an indirect indication of strong metal-support interaction. For Pd/Zr-Lap and Pd/Ce-Lap catalysts, the elevated calcination temperature weaken the metal-support interaction because the particle size becomes larger and reaches a desirable value. Regarding Pd/Al-Lap catalysts, calcination at  $400\text{ }^\circ\text{C}$  seemed to be the optimal condition for the formation of a catalyst with palladium crystallites of a desirable size.

### 3.5. Comparison of the catalytic activity of palladium catalysts loaded on various supports

The ignition curves for benzene deep oxidation over various types of catalysts were compared in Fig. 6. The destruction efficiency of all the three types of pillared clays supported catalysts, which were all capable of achieving total conversion of benzene at less than  $300\text{ }^\circ\text{C}$ , were far more superior to both alumina and the parent clay supported catalysts. In particular, Pd/Zr-Lap(600–500) appeared to be the most active catalyst with a very steep conversion curve, on which the oxidation of benzene became appreciable at  $140\text{--}150\text{ }^\circ\text{C}$ , approaching 50% of conversion at  $180\text{ }^\circ\text{C}$  and quickly reaching complete conversion at  $210\text{ }^\circ\text{C}$ . But, in the case of conventional Pd/Al<sub>2</sub>O<sub>3</sub> catalyst, the reaction started at  $200\text{ }^\circ\text{C}$  and complete combustion was not achieved until the temperature was raised to  $410\text{ }^\circ\text{C}$ . The activity of the pillared clays supported palladium catalysts were in the following descending order with respect to the pillar composition: Zr-Lap > Ce-Lap > Al-Lap. Apparently, the order of catalytic activity does not follow the order of the specific surface areas of the catalysts (Table 2). The nature of the pillar compositions might play a more important role in determining the catalytic activity. Zirconia appeared to be the most efficient promoter toward benzene oxidation. Zirconia could act as an acid–base bifunctional catalyst exhibiting higher activity for C–H bond cleavage than strong acidic SiO<sub>2</sub>–Al<sub>2</sub>O<sub>3</sub> and

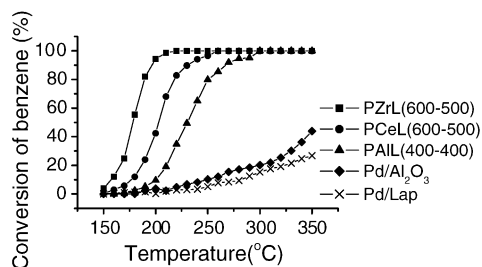


Fig. 6. Conversion curves for benzene oxidation over palladium catalysts loaded on various supports.

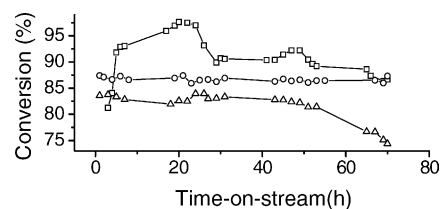


Fig. 7. Stability tests of benzene conversion with time-on-stream over various catalysts. (○): PZrL(600–500) at  $200\text{ }^\circ\text{C}$ ; (□): PAIL(400–400) at  $220\text{ }^\circ\text{C}$ ; (△): PCeL(600–500) at  $235\text{ }^\circ\text{C}$ .

Al<sub>2</sub>O<sub>3</sub> or strongly acidic solids [13,39]. And the C–H cleavage has been reported to be the initial step of hydrocarbon oxidation [27,40]. Meanwhile, Zr induced weakening of the Pd–O bond due to its weak basic property, thus favoring the C–H activation step [41]. In addition, the oxygen mobility of zirconia is rather high [28,42], thus promotes the interaction with the hydrocarbon fragments [43,44].

### 3.6. Long-term stability tests

A series of long-term stability tests over the three types of pillared clays supported catalysts were performed to evaluate the stability of the catalytic activity. And the evolutions of benzene conversion with time-on-stream are shown in Fig. 7. The conversion of benzene over Pd/Zr-Lap catalyst was well sustained at about  $86.7\%$  ( $\pm 0.7\%$ ) for 70 h, and no noticeable deactivation was observed. In contrast, the activity of Pd/Ce-Lap was sustained at about  $83\%$  ( $\pm 0.8\%$ ) only for the first 50 h, then it began to decrease, and the conversion value fell down to about  $74.5\%$  after 70 h. Regard to Pd/Al-Lap catalyst, the conversion value increased to  $97\%$  in the first 20 h, then gradually decreased to about  $91\%$  ( $\pm 1\%$ ), further decrease began after the test run had been operated for about 50 h, and the conversion value after 70 h was about  $86.5\%$ .

## 4. Conclusions

The laponite clay was modified by pillaring with alumina, ceria and zirconia. The specific surface areas of all the pillared clays exceed  $430\text{ m}^2/\text{g}$ , and the pore diameters are larger than 4 nm. The pillaring process enhanced the thermal stability of the clay, especially for the Zr-pillared clay. The calcination temperatures affected significantly the activity of the pillared clays supported palladium catalysts. For the Pd/Al-Lap series of catalysts,  $400\text{ }^\circ\text{C}$  appeared to be the optimal calcination temperature, while for the Pd/Ce-Lap and Pd/Zr-Lap series of catalysts, calcination temperature higher than  $600\text{ }^\circ\text{C}$  were required to generate the best activity. At optimal calcination temperatures, palladium crystallites of proper size could be formed in pillared clays. Pd/Zr-Lap, which converts benzene completely at less than  $210\text{ }^\circ\text{C}$ , appeared to be the most active catalyst. Pd/Zr-Lap showed an excellent stability of the catalytic performance during a long-term stability test of 70 h.

## Acknowledgements

Financial funds from the Knowledge Innovation Funds of the Chinese Academy of Sciences (key project KZCX3-SW-430), the Chinese Natural Science Foundation (project no. 20322201) and the Asian Regional Research Programme on Environmental Technology (ARRPET) sponsored by the Swedish International Development for Research Cooperation Agency (Sida) are gratefully acknowledged.

## References

- [1] J.A. Horsley, Catalytic Environmental Report E4, Catalytic Studies Division, Mountain View, CA, USA, 1993.
- [2] J.J. Spivey, *Ind. Eng. Chem. Res.* 26 (1987) 2165.
- [3] G. Centi, P. Ciambelli, S. Perathoner, P. Russo, *Catal. Today* 75 (2002) 3.
- [4] S. Wang, H.Y. Zhu, G.Q. Lu, *J. Colloid Interface Sci.* 28 (1998) 204.
- [5] H.Y. Zhu, S. Yamanaka, *Faraday Trans.* 93 (1997) 477.
- [6] A. Gil, L.M. Gandia, M.A. Vicente, *Catal. Rev.: Sci. Eng.* 42 (2000) 145.
- [7] H.Y. Zhu, G.Q. Lu, *Langmuir* 17 (2001) 588.
- [8] H.Y. Zhu, Z.P. Hao, J.C. Barry, *Chem. Commun.* (2002) 2858.
- [9] Z.P. Hao, H.Y. Zhu, G.Q. Lu, *Appl. Catal. A* 242 (2003) 275.
- [10] S. Moreno, R. Sun Kou, G. Poncelet, *J. Phys. Chem. B* 101 (1997) 1569.
- [11] A.M. Pisanu, C.E. Gigola, *Appl. Catal. B* 11 (1996) 37.
- [12] J. Anderson, *Structure of Metallic Catalysts*, Academic Press, New York, 1975, p. 296.
- [13] L.M. Gandía, M.A. Vicente, A. Gil, *Appl. Catal. B* 38 (2002) 295.
- [14] M.A. Vicente, M.A. Bañares-Muñoz, L.M. Gandía, A. Gil, *Appl. Catal. A* 217 (2001) 191.
- [15] D. Martin, D. Duprez, *J. Phys. Chem. B* 101 (1997) 4428.
- [16] E. Marceau, M. Che, J. Saint-Just, J.M. Tatibouët, *Catal. Today* 29 (1996) 415.
- [17] H. Windawi, Z.C. Zhang, *Catal. Today* 30 (1996) 99.
- [18] N.W. Cant, D.E. Angove, M.J. Patterson, *Catal. Today* 44 (1998) 93.
- [19] F. Giordano, A. Trovarelli, C. De Leitenburg, M. Giona, *J. Catal.* 193 (2003) 273.
- [20] P. Fornasiero, J. Kaspar, M. Graziani, *J. Catal.* 167 (1997) 576.
- [21] A. Trovarelli, G. Dolcetti, C. De Leitenburg, J. Kaspar, P. Finetti, A. Santoni, *J. Chem. Soc., Faraday Trans.* 88 (1992) 1311.
- [22] H.C. Yao, Y.F. Yao, *J. Catal.* 86 (1984) 254.
- [23] S. Scirè, S. Minicò, C. Crisafulli, C. Satriano, A. Pistone, *Appl. Catal. B* 40 (2003) 43.
- [24] M.-F. Luo, X.-M. Zheng, *Appl. Catal. A* 189 (1999) 15.
- [25] C.K. Shi, L.F. Yang, Z.C. Wang, X.E. He, J.X. Cai, G. Li, X.S. Wang, *Appl. Catal. A* 243 (2003) 379.
- [26] P. Fornasiero, R. Di Monte, G. Ranga Rao, J. Kaspar, A. Trovarelli, M. Graziani, *J. Catal.* 151 (1995) 168.
- [27] G. Busca, E. Finocchio, V. Lorenzelli, G. Ramis, M. Baldi, *Catal. Today* 49 (1999) 453.
- [28] S. Yang, A. Maroto-Valiente, M. Benito-Gonzalez, I. Rodriguez-Ramos, A. Guerrero-Ruiz, *Appl. Catal. B* 28 (2000) 223.
- [29] L. Becker, H. Förster, *Appl. Catal. B* 17 (1998) 43.
- [30] C.A. Müller, M. Maciejewski, R.A. Koeppl, A. Baiker, *Catal. Today* 47 (1999) 245.
- [31] Y. Yazawa, H. Yoshida, N. Takagi, S. Komai, A. Satsuma, T. Hattori, *J. Catal.* 187 (1999) 15.
- [32] W.S. Epling, G.B. Hoflund, *J. Catal.* 182 (1999) 5.
- [33] Lj. Kundakovic, M. Flytzani-Stephanopoulos, *Appl. Catal. A* 171 (1998) 13.
- [34] A.Y. Khodakov, A. Griboval-Constant, R. Bechara, F. Villain, *J. Phys. Chem. B* 105 (2001) 9805.
- [35] A.Y. Khodakov, J. Lynch, D. Bazin, B. Rebours, N. Zanier, B. Moisson, P. Chaumette, *J. Catal.* 168 (1997) 16.
- [36] R. Bechara, D. Balloy, J.Y. Dauphin, J. Crimblot, *Chem. Mater.* 11 (1999) 1703.
- [37] C.M. Pradier, F. Rodrigues, P. Marcus, M.V. Landau, M.L. Kaliya, A. Gutman, M. Herskowitz, *Appl. Catal. B* 27 (2000) 73.
- [38] L. Ji, J. Lin, H.C. Zeng, *J. Phys. Chem. B* 104 (2000) 1783.
- [39] K. Tanaka, M. Misono, Y. Ono, H. Hattori, *New Solid Acid and Based: Their Catalytic Properties*, Elsevier, Amsterdam, 1989, p. 55.
- [40] R. Burch, D.J. Crittle, M.J. Hayes, *Catal. Today* 47 (1999) 229.
- [41] R.W. van den Brink, R. Louw, P. Mulder, *Appl. Catal. B* 25 (2000) 229.
- [42] D. Duprez, *Stud. Surf. Sci. Catal.* 112 (1997) 13.
- [43] E. Finocchio, R.J. Willey, G. Ramis, *Stud. Surf. Sci. Catal.* 101 (1996) 483.
- [44] J. Haber, *Stud. Surf. Sci. Catal.* 110 (1997) 1.